

Fermi National Accelerator Laboratory

FERMILAB-Pub-94/076-E

E687

Analysis of Three $D \rightarrow K \pi \pi$ Dalitz Plots

P.L. Frabetti et al
The E687 Collaboration

*Fermi National Accelerator Laboratory
P.O. Box 500, Batavia, Illinois 60510*

March 1994

Submitted to *Physics Letters B*

Disclaimer

This report was prepared as an account of work sponsored by an agency of the United States Government. Neither the United States Government nor any agency thereof, nor any of their employees, makes any warranty, express or implied, or assumes any legal liability or responsibility for the accuracy, completeness, or usefulness of any information, apparatus, product, or process disclosed, or represents that its use would not infringe privately owned rights. Reference herein to any specific commercial product, process, or service by trade name, trademark, manufacturer, or otherwise, does not necessarily constitute or imply its endorsement, recommendation, or favoring by the United States Government or any agency thereof. The views and opinions of authors expressed herein do not necessarily state or reflect those of the United States Government or any agency thereof.

Analysis of Three $D \rightarrow K\pi\pi$ Dalitz Plots

E687 Collaboration

P. L. Frabetti

Dip. di Fisica dell'Università and INFN - Bologna, I-40126 Bologna, Italy

H. W. K. Cheung [a], J. P. Cumalat, C. Dallapiccola [b], J. F. Ginkel, S. V. Greene,

W. E. Johns, M. S. Nehring

University of Colorado, Boulder, CO 80309, USA

J. N. Butler, S. Cihangir, I. Gaines, P. H. Garbincius, L. Garren, S. A. Gourlay,

D. J. Harding, P. Kasper, A. Kreymer, P. Lebrun, S. Shukla, M. Vittone

Fermilab, Batavia, IL 60510, USA

S. Bianco, F. L. Fabbri, S. Sarwar, A. Zallo

Laboratori Nazionali di Frascati dell'INFN, I-00044 Frascati, Italy

R. Culbertson, R. W. Gardner, R. Greene, J. Wiss

University of Illinois at Urbana-Champaign, Urbana, IL 61801, USA

G. Alimonti, G. Bellini, B. Caccianiga, L. Cinquini [c], M. Di Corato, M. Giammarchi,

P. Inzani, F. Leveraro, S. Malvezzi [d], D. Menasce, E. Meroni, L. Moroni, D. Pedrini,

L. Perasso, A. Sala, S. Sala, D. Torretta [a]

Dip. di Fisica dell'Università and INFN - Milano, I-20133 Milan, Italy

D. Buchholz, D. Claes [e], B. Gobbi, B. O'Reilly,

Northwestern University, Evanston, IL 60208, USA

J. M. Bishop, N. M. Cason, C. J. Kennedy [f], G. N. Kim [g], T. F. Lin, D. L. Puseljic [h],

R. C. Ruchti, W. D. Shephard, J. A. Swiatek, Z. Y. Wu

University of Notre Dame, Notre Dame, IN 46556, USA

V. Arena, G. Boca, C. Castoldi, G. Gianini, S. P. Ratti, C. Riccardi, P. Vitulo

Dip. di Fisica Nucleare e Teorica and INFN - Pavia, I-27100 Pavia, Italy

A. Lopez, University of Puerto Rico at Mayaguez, Puerto Rico

G. P. Grim, V. S. Paolone, P. M. Yager, University of California-Davis, Davis, CA 95616, USA

J. R. Wilson, University of South Carolina, Columbia, SC 29208, USA

P. D. Sheldon, Vanderbilt University, Nashville, TN 37235, USA

F. Davenport, University of North Carolina-Asheville, Asheville, NC 28804, USA

G.R. Blakett, M. Pisharody, T. Handler

University of Tennessee, Knoxville, TN 37996, USA

B. G. Cheon, J. S. Kang, K. Y. Kim

Korea University, Seoul 136-701, Korea

Abstract

Analysis of three $D \rightarrow K\pi\pi$ Dalitz plots is presented using data collected by the Fermilab high energy photoproduction experiment E687. Our data are fit to a model consisting of a sum of Breit-Wigner amplitudes for the intermediate two-body resonant decay modes and a constant term for the nonresonant contribution. We extract branching fractions and relative phases and compare them to the results obtained in other experiments. Although this model qualitatively reproduces many features of our data, statistically significant discrepancies are observed in some of our fits.

Typeset using REVTeX

The nonleptonic decays of D mesons are an important source of information for understanding various experimental facts in charmed particle decay such as the lifetime difference between the D^+ and D^0 mesons. Models of nonleptonic D decay [1] which attempt to explain such phenomena can be tested by comparing the predicted pattern of exclusive decay channels against experiment. Measurements of the three-body final states of D mesons to determine resonant two-body branching fractions as well as the direct three-body nonresonant component have been previously reported [2–5]. Here we present a high sensitivity Dalitz plot analysis of the final states* $D^0 \rightarrow K_s^0 \pi^+ \pi^-$, $D^+ \rightarrow K^- \pi^+ \pi^+$, and $D^0 \rightarrow K^- \pi^+ \pi^0$ using data collected by the Fermilab photoproduction experiment E687.

The E687 spectrometer has good detection capabilities for leptons, charged hadrons, and photons. Charged particles emerging from photon-Beryllium target interactions are tracked by a microvertex detector consisting of 12 planes of silicon microstrips which allow secondary vertices to be separated from the primary (production) vertex. Downstream deflections by two analysis magnets of opposite polarity are measured by five stations of proportional wire chambers (PWCs). Pions and kaons are identified by three multicell Čerenkov counters operating in threshold mode. Identification of π^0 candidates is accomplished with electromagnetic calorimeter modules consisting of lead-scintillator sandwich detectors configured in three measurement views. A detailed description of the E687 apparatus, beam, and trigger conditions can be found elsewhere [6].

The $D^0 \rightarrow K_s^0 \pi^+ \pi^-$ events were selected in a manner similar to our previous analysis of this mode [3] which used data collected from the 1987-88 run of E687. In the present analysis, owing to the larger data sample and the desire to further reduce background, the D^0 was required to be produced from the decay reaction $D^{*+} \rightarrow D^0 \pi^+$. This also provides a tag of the strangeness quantum number of the observed K_s^0 (and thus the charm quantum

*Throughout this paper, when referencing a particular state we implicitly include its charge conjugate.

number of the parent D^0/\overline{D}^0) which was identified by its decay mode $K_s^0 \rightarrow \pi^+\pi^-$. The K_s^0 is combined with pairs of oppositely charged tracks found by both microstrip and PWC systems to form a D^0 candidate. In order to improve the signal-to-background ratio, the $K_s^0\pi^+\pi^-$ combination was required to have momentum greater than 45 GeV/c. The pion candidates from the D^0 vertex were required to have Čerenkov light patterns consistent with the pion hypothesis. These tracks, together with the K_s^0 candidate, were tested to form a common secondary vertex with a confidence level exceeding 1%. The primary vertex was searched for using a seed track reconstructed from the D^0 candidate momentum vector and the secondary vertex point. Remaining tracks in the event which intersected the seed track and each other with acceptable confidence level were considered primary vertex tracks. The primary vertex candidate was required to have at least two tracks in addition to the seed track. The secondary vertex was required to be downstream of the primary vertex by at least 5 standard deviations[†] ($\ell > 5\sigma_\ell$). To ensure the secondary vertex was well isolated, leftover tracks not found in the primary vertex were required to be inconsistent with emerging from the secondary vertex and secondary tracks were required not to point to the primary vertex. We required the $D^{*+} - D^0$ mass difference to lie within 2 MeV/c² of the accepted value [7], and the associated π^+ from the D^{*+} decay be found in the primary vertex. To remove possible contamination from the decay mode $D^0 \rightarrow \pi^+\pi^+\pi^-\pi^-$, we required the K_s^0 vertex to be downstream of the D^0 vertex by at least 3 standard deviations. The resulting invariant mass spectrum for $D^0 \rightarrow K_s^0\pi^+\pi^-$ candidates satisfying these cuts is shown in Fig. 1(a). The yield of events from a fit to a Gaussian distribution plus a linear function to account for background is 597 ± 26 with a very high signal-to-background ratio. Events having $M(K_s^0\pi^+\pi^-)$ in the region $\pm 2\sigma$ from the signal peak ($\sigma = 12.4$ MeV/c²) were selected for the Dalitz plot fit. Events from the sidebands (4σ width separated by 2σ below and above

[†]The variable ℓ is the signed 3 dimensional separation between vertices and σ_ℓ is the error on ℓ computed on an event-by-event basis including effects of multiple Coulomb scattering.

the signal region) were used to characterize the background in the signal region, as discussed below.

For the decay mode $D^+ \rightarrow K^-\pi^+\pi^+$ the most significant requirements were $\ell > 20\sigma_\ell$, that the kaon track be identified as a kaon or kaon-proton ambiguous, that the pions were inconsistent with being either kaons or protons, and that the vertex was well isolated. Contamination from decay $D^{*+} \rightarrow D^0\pi^+$, $D^0 \rightarrow K^-\pi^+\pi^0$ is limited to a very small region of the $D^+ \rightarrow K^-\pi^+\pi^+$ phase space at low $m^2(\pi\pi)$ and $m^2(K\pi)$ which was excluded from the analysis. The resulting invariant mass spectrum is shown in Fig. 1(b). The yield of events from a fit to a Gaussian distribution plus a linear background function is 8800 ± 97 with $\sigma = 11.3 \text{ MeV}/c^2$. Events from the sidebands were used to characterize the background in the signal region.

Candidates for the decay $D^0 \rightarrow K^-\pi^+\pi^0$, produced from the decay reaction $D^{*+} \rightarrow D^0\pi^+$, were selected from a pre-skimmed sample which required the evidence of detached vertices in the event. Specifically, all high-quality two-track vertices were formed and the event was accepted if any two two-track vertices were separated by more than 4.5σ . For the π^0 candidates, pairs of neutral showers reconstructed by the inner electromagnetic calorimeter (covering approximately ± 28 and ± 47 mrad in the x and y views) were required to be outside of the spectrometer centerline by 6 cm in the x view (corresponding to the region of beam related Bethe-Heitler pairs), and to have $0.09 < M(\pi^0) < 0.16 \text{ GeV}/c^2$. The kaon track was required to be consistent with the kaon hypothesis or kaon-pion ambiguous if its momentum was greater than 61 GeV/c (corresponding to the highest kaon threshold momentum of the Čerenkov system). The $K^-\pi^+\pi^0$ combinations were required to have momentum greater than 70 GeV/c which improved the signal-to-background ratio. We applied the same $D^{*+} - D^0$ mass difference cut as for the decay mode $D^0 \rightarrow K_s^0\pi^+\pi^-$, and also required the D^{*+} -associated π^+ be found in the primary vertex. We required the secondary vertex to be downstream from a primary vertex candidate (formed by at least two tracks in addition to the seed track) by $\ell > 5\sigma_\ell$ and to be well isolated. Because the invariant mass resolution of the $K^-\pi^+\pi^0$ combination is a strong function of the fraction of

the D^0 energy carried by the π^0 , we select events based on their *normalized* invariant mass[‡] $(M(K^-\pi^+\pi^0) - M_{D^0})/\sigma$, which we require to be less than 2 for the Dalitz plot fit. In figure Fig. 1(c) we plot the normalized invariant mass for combinations having the correct charge correlation between the kaon and D^{*+} -associated π^+ . The curve shown is a fit to a Gaussian distribution and a linear background function from which the yield of events is 530 ± 30 . Events with the incorrect charge correlation are shown by the dashed histogram and are used to estimate the background shape for the correct charge events.

Following our previous work [3], we performed maximum likelihood fits to the three $D \rightarrow K\pi\pi$ Dalitz plots to measure the decay fractions into the intermediate modes as well as their relative phases. In the present analysis we have extended the formalism to allow for the possibility of contributions from all known $(K\pi)$ and $(\pi\pi)$ resonances [7]. The total decay amplitude for a $D \rightarrow K\pi\pi$ decay is assumed to consist of a flat, uniform term for the three-body nonresonant contribution plus a sum of functions B which represent intermediate strong resonances and decay angular momentum conservation. The fit parameters[§] are amplitude coefficients a_i and phases δ_i :

$$\mathcal{A}(D) = a_0 e^{i\delta_0} + \sum_i a_i e^{i\delta_i} B(a b c |r). \quad (1)$$

Explicitly, a, b , and c label the final state particles, $B(a b c |r) = BW(a, b|r) \mathcal{S}(a, c)$ where $BW(a, b|r)$ is the Breit-Wigner function**

[‡] σ is the error on $M(K^-\pi^+\pi^0)$ computed on an event-by-event basis and on average is approximately 20 MeV/ c^2 . The value for M_{D^0} is taken from reference [7].

[§]We fix the parameters of the dominant decay mode to have amplitude coefficient $a_i = 1$ and phase $\delta_i = 0$.

**In order to compare our results to Ref. [5], we have used the Blatt-Weisskopf penetration factors F_D and F_r ; however the dependence of all results on these factors was found to be small and are included in the systematic errors. For each resonance of mass M_r and spin j we use a width Γ

$$BW(a, b|r) = \frac{F_D F_r}{M_r^2 - M_{ab}^2 - i \Gamma M_r} \quad (2)$$

and, $\mathcal{S}(a, c) = 1$ for a spin 0 resonance, $\mathcal{S}(a, c) = (-2 \vec{c} \cdot \vec{a})$ for a spin 1 resonance, and $\mathcal{S}(a, c) = 2(|\vec{c}||\vec{a}|)^2(3 \cos^2 \theta^* - 1)$ for a spin 2 resonance.^{††} The \vec{c} and \vec{a} are the three momenta of particles c and a measured in the ab rest frame, and $\cos \theta^* = \vec{c} \cdot \vec{a} / |\vec{c}||\vec{a}|$.

We emphasize that the order of particle labels implies our convention of relative phase (eg. interchanging a and b results in phase shift of 180 degrees for the vector modes), and thus we specify them here. For the $D^0 \rightarrow K_s^0 \pi^+ \pi^-$ final state, $B(a b c|r)$ was computed according to $B(K_s^0 \pi^- \pi^+ |(K\pi))$ for $(K\pi)$ resonances and $B(\pi^+ \pi^- K_s^0 |(\pi\pi))$ for $(\pi\pi)$ resonances. For the $D^0 \rightarrow K^- \pi^+ \pi^0$ final state, two charge states are possible for $(K\pi)$ resonances and we used $B(K^- \pi^+ \pi^0 |(K\pi)^{*0})$ and $B(K^- \pi^0 \pi^+ |(K\pi)^{* -})$, while $B(\pi^+ \pi^0 K^- |(\pi\pi))$ was used for the $(\pi\pi)$ resonances. For the $D^+ \rightarrow K^- \pi^+ \pi^+$ final state, $(K\pi)$ amplitudes were Bose-symmetrized by computing $B(K^- \pi_1^+ \pi_2^+ |(K\pi)) + B(K^- \pi_2^+ \pi_1^+ |(K\pi))$.

The amplitudes were weighted by a function to correct for geometrical acceptance and reconstruction efficiency; biases caused by finite spectrometer mass resolution were small for the $D^0 \rightarrow K_s^0 \pi^+ \pi^-$ and $D^0 \rightarrow K^- \pi^+ \pi^-$ modes. For the $D^0 \rightarrow K^- \pi^+ \pi^0$ final state, the amplitude, expressed as a function of the invariant mass-squared variables $m^2(K^- \pi^0)$ and $m^2(K^- \pi^+)$, was weighted by a Gaussian resolution function (determined by Monte Carlo) over the $m^2(K^- \pi^0)$ projection with $\sigma = 0.025 \text{ GeV}^2/c^4$.

To account for the background contribution we used two methods. In the first method we directly subtracted the likelihood using the events in the D sidebands for the $D^0 \rightarrow K_s^0 \pi^+ \pi^-$ and $D^+ \rightarrow K^- \pi^+ \pi^+$ modes, and wrong-sign events for the $D^0 \rightarrow K^- \pi^+ \pi^0$ mode. This method avoids any dependence on a background model or parameterization. In the

which is proportional to $p^{2j+1} F_r^2 / M_{ab}$ where p is the decay momentum in the resonance rest frame.

^{††}We searched for decays through intermediate resonances of spin 3 and spin 4 but found insignificant contributions from those modes.

second method we first performed fits to the sideband Dalitz plots using uniformly populated Breit-Wigner bands and polynomial functions of the mass-squared variables. The resulting parameterized background shapes were used to describe background events in the signal region, and we allowed these parameters to vary within their errors during the fit. In most cases the methods produced equivalent results; in the following we quote only the results using the second method and attribute any differences to systematic errors.

A likelihood function consisting of signal and background probability densities was maximized over the variables a_i and δ_i for each $D \rightarrow K\pi\pi$ final state. The Dalitz plot distributions, mass-squared projections, and fit results are illustrated in Figs. 2-3. In these figures the fit predictions are compared to the data by integrating the probability density over strips in the Dalitz plot corresponding to the bins in the mass-squared projections. The fitted decay fractions and relative phases are summarized in Tables I-III. The decay fraction into a given mode was computed by integrating the signal intensity for that mode alone divided by the integrated intensity with all modes present.^{††} These fractions do not sum to one due to the presence of interference between the modes. The branching ratios are computed by multiplying the decay fraction by the branching ratio for the three-body final state [7], and dividing by the branching ratio for the $(K\pi)$ or $(\pi\pi)$ resonance where appropriate.

The number of possible $(K\pi)$ and $(\pi\pi)$ resonances is quite large and many of these have poorly measured resonance parameters [7]. Some decay channels leave clearly evident “landmarks” in the mass-squared projections, while the signature from others (such as those with large width) is much less visible. In the fit results shown we have required that each hypothesized decay mode contribute with a decay fraction of at least 2.5 standard deviations to be included in the final result. The fit quality was evaluated in two ways. In the first

^{††}This definition, which has become conventional, allows direct comparison of fit results which are independent of the choice of amplitude formalism.

method, which was used by Ref. [5], we computed a confidence level using the final value of the likelihood function from the fit and a table of likelihood values derived from repeated Monte Carlo simulations of the experiment assuming as input our final fit result. All fits discussed in this paper returned a confidence level exceeding 10% using this method. In the second method we calculated a $\chi^2/(\text{dof})$ value by comparing the two-dimensional Dalitz plot distribution to the probability function integrated over bins chosen adaptively such that the predicted and observed number of events in each comparison bin were at least 10 events for the $D^0 \rightarrow K^-\pi^+\pi^0$ and $D^0 \rightarrow K_s^0\pi^+\pi^-$ final states and at least 150 events for the (high statistics) $D^+ \rightarrow K^-\pi^+\pi^+$ final state. For high statistics data sets, the second method is often the more stringent criteria for goodness-of-fit since variations along the constant likelihood intensity contour are also tested. This method reveals statistically significant discrepancies in the $D^0 \rightarrow K_s^0\pi^+\pi^-$ and $D^+ \rightarrow K^-\pi^+\pi^+$ Dalitz plot fits.

The systematic errors in the decay fractions and phases reflect uncertainties in reconstruction efficiency and background subtraction methods. For example, we split our data samples into high and low momentum events, into particle and anti-particle samples, and we varied the background subtraction technique and the predicted background level in the fit. Checks of the fitting procedure were made using Monte Carlo techniques and all biases were found to be small compared to the statistical errors. We considered various mass dependent forms for the Breit-Wigner amplitudes [8] and have included any variations in the quoted errors. A large source of systematic error in some of the parameters arises from which ($K\pi$) and ($\pi\pi$) resonances contribute to the final state and from the uncertainties in the ($K\pi$) and ($\pi\pi$) resonance shapes themselves [7]; the third set of error bars in the tables reflect uncertainties of this type.^{§§}

Our result for the $D^0 \rightarrow K_s^0\pi^+\pi^-$ final state, as indicated by the comparison between the

^{§§}We varied the resonance parameters by $\pm 1\sigma$ about the central mass values and widths as given in Ref. [7].

fit prediction and the data in the mass-squared projection histograms of Fig. 2, suggests the decay can be *approximately* described by a sum of intermediate two-body resonant decay modes.** However, the overall fit quality is not very good as the $\chi^2/(\text{dof})$, computed over adaptively chosen bins in the two-dimensional Dalitz plot, has the unacceptable value of 2.29 for 23 degrees of freedom. The bins which showed the largest disagreement were in the K^{*-} Breit-Wigner peak and had $m_{\pi^+\pi^-}^2$ between 1.2 and 1.6 GeV^2/c^4 , corresponding to the region where interference contributions between the $D^0 \rightarrow K^{*-}\pi^+$ decay mode and other decay modes would naturally be evident. This may be suggestive of strong-interaction dynamics not contained in the model we have assumed in this analysis such as the presence of new, undiscovered wide resonances or a non-uniform, nonresonant amplitude with possible varying phase.

The $D^+ \rightarrow K^-\pi^+\pi^+$ decay mode is characterized by a large nonresonant contribution. We attempted but failed to fit the Dalitz plot using an exclusive sum of intermediate two-body decay modes formed with any combination of the known $(K\pi)$ resonances. Our best fit assumes a uniform amplitude for the nonresonant contribution which is added coherently to the $(K\pi)$ resonant modes. In this fit, there are clearly evident discrepancies in the comparison of the fit prediction and mass-squared projection histograms as shown in Fig. 2. The χ^2 test computed over the two-dimensional Dalitz plot distribution yields $\chi^2/(\text{dof}) = 3.01$ for 29 degrees of freedom.

The $D^0 \rightarrow K^-\pi^+\pi^0$ final state is best described by a sum of intermediate two-body resonances (with $D^0 \rightarrow K^-\rho^+$ as the dominant decay mode) plus a relatively small non-

***We note that our previous analysis of the $D^0 \rightarrow K_s^0\pi^+\pi^-$ final state [3], owing to the smaller data sample collected in the first run of our experiment, assumed only three contributing decay modes: the dominant $D^0 \rightarrow K^{*-}\pi^+$ and $D^0 \rightarrow \overline{K^0}\rho^0$ modes and the three-body nonresonant mode. When our present data sample was fit under the original assumptions we reproduced our earlier measurements within errors.

resonant component (decay fraction = 0.101 ± 0.033) as illustrated in Fig. 3. The χ^2 test computed over the two-dimensional Dalitz plot distribution yields an acceptable value of $\chi^2/(\text{dof}) = 1.59$ for 24 degrees of freedom. We note that the $D^0 \rightarrow K^{*-}\pi^+$ branching ratio is in good agreement with that measured in the $D^0 \rightarrow K_s^0\pi^+\pi^-$ final state. With the present statistics we cannot rule out contributions from additional higher mass and spin ($K\pi$) and ($\pi\pi$) resonances; such resonances would tend to diminish the three-body nonresonant decay fraction.

In Tables IV and V we compare the results of our analysis to other experiments. Our branching ratios for the $D^0 \rightarrow K_s^0\pi^+\pi^-$ final state are in good agreement with those of Ref. [5]. In particular, both experiments find the final state to be largely dominated by two decay modes, $D^0 \rightarrow K^{*-}\pi^+$ and $D^0 \rightarrow \overline{K^0}\rho^0$. Additionally, the agreement between relative phase measurements is quite good!^{††} In our fit we have assumed a contribution from the $f_0(1400)$ resonance, which is a broad scalar resonance with poorly known resonance parameters [7]. If this resonance is replaced by a flat, coherent 3-body amplitude, we find an acceptable fit to our data with a 3-body decay fraction of 0.102 ± 0.036 and relative phase of -32 ± 11 degrees.

For the $D^0 \rightarrow K^-\pi^+\pi^0$ and $D^+ \rightarrow K^-\pi^+\pi^+$ modes, our results for the branching ratios are in fair agreement with results from Refs. [2,4], while most of the relative phase measurements appear to show significant disagreement. We point out, however, that when the results from Ref. [4] are shifted by $\pm 90^\circ$, which could result from an extra factor of i in their (unspecified) Breit-Wigner propagators, some results are in better agreement.

^{†††}We note that when the authors of Ref. [5] fit their data using the assumptions of our first analysis [3], their results are consistent with our earlier work [3] with the possible exception of the three-body nonresonant phase. However, comparison of our amplitude expression and that found in Ref. [5] indicates that when the difference in Breit-Wigner convention is accounted for the result for this phase is in better agreement than suggested by Tables 1 and 2 of Ref. [5].

A possible difference in phase convention may also account for our discrepancy with the relative phase of the $D^0 \rightarrow K^-\pi^+\pi^0$ three-body amplitude measured by Ref. [2]; our value is in good agreement with theirs if 180 degrees are added to either result.

Using our results for the branching fractions into the modes $D^0 \rightarrow K^{*-}\pi^+$, $D^0 \rightarrow \overline{K}^{*0}\pi^0$, and $D^+ \rightarrow \overline{K}^{*0}\pi^+$ and assuming quasi-stable two-body decay, we can compute the $I = 1/2$ and $I = 3/2$ isospin amplitudes in the $D \rightarrow K^*\pi$ system [9]. We find $|A_{1/2}|/|A_{3/2}| = 5.9 \pm 0.3 \pm 0.3$, which is somewhat larger than values obtained by previous experiments [2,4] and the values reported for $D \rightarrow K\pi$ and $D \rightarrow K\rho$ decays [2]. A relative phase shift between the isospin amplitudes is caused by final state interactions. Our measurement of the phase shift, $\delta_{1/2} - \delta_{3/2} = 95 \pm 16 \pm 21^\circ$, is in agreement with previous results [2,4].

In summary, our fits to three $D \rightarrow K\pi\pi$ Dalitz distributions assuming a model with Breit-Wigner amplitudes for the two-body resonant modes and a constant term for the three-body nonresonant channel qualitatively reproduce many features of our data, although statistically significant discrepancies are observed in two of our fits. While intermediate two-body resonant modes dominate the decays $D^0 \rightarrow K_s^0\pi^+\pi^-$ and $D^0 \rightarrow K^-\pi^+\pi^0$, the decay $D^+ \rightarrow K^-\pi^+\pi^+$ can not be satisfactorily described without a large nonresonant contribution. Our branching fraction measurements are in fair agreement with other experiments as are the relative phases if differences in amplitude convention are accounted for. Our result for the phase difference between the $I = 1/2$ and $I = 3/2$ isospin amplitudes affirms the importance of final state interactions in charm decays.

We wish to acknowledge the assistance of the staffs of the Fermi National Accelerator Laboratory, the INFN of Italy, and the physics departments of the collaborating institutions. This research was supported in part by the National Science Foundation, the U.S. Department of Energy, the Italian Istituto Nazionale di Fisica Nucleare and Ministero dell'Università e della Ricerca Scientifica e Tecnologica, and the Korean Science and Engineering Foundation.

REFERENCES

- ^a Present address: Fermilab, Batavia, IL 60510, USA.
- ^b Present address: University of Maryland, College Park, MD 20742, USA.
- ^c Present address: University of Colorado, Boulder, CO 80309, USA.
- ^d Present address: Dip. di Fisica Nucleare e Teorica and INFN - Pavia, I-27100 Pavia, Italy.
- ^e Present address: University of New York, Stony Brook, NY 11794, USA.
- ^f Present address: Yale University, New Haven, CN 06511, USA.
- ^g Present address: Pohang Accelerator Laboratory, Pohang, Korea.
- ^h Present address: Lawrence Berkeley Laboratory, University of California, Berkeley, CA 94720, USA.
- ¹ See for example the following and references therein:
M. Bauer, B. Stech, M. Wirbel, *Z. Phys. C* 34 (1987) 103;
B. Yu. Blok, M.A. Shifman, *Sov. J. Nucl. Phys.* 45 (1987) 522;
L.L. Chau, H.Y. Cheng, *Phys. Rev. D* 36 (1987) 137;
M. Diakonou and F. Diakonov, *Phys. Lett. B* 216 (1989) 436;
P. Bedaque, A. Das, V.S. Mathur, *Phys. Rev. D* 49 (1994) 269.
- ² Mark III Collab., J. Adler *et al.*, *Phys. Lett. B* 196 (1987) 107.
- ³ E687 Collab., P.L. Frabetti *et al.*, *Phys. Lett. B* 286 (1992) 195.
- ⁴ E691 Collab., J.C. Anjos *et al.*, *Phys. Rev. D* 48 (1993) 56.
- ⁵ ARGUS Collab., H. Albrecht *et al.*, *Phys. Lett. B* 308 (1993) 435.
- ⁶ E687 Collab., P.L. Frabetti *et al.*, *Nucl. Instrum. Methods. A* 320 (1992) 519;
E687 Collab., P.L. Frabetti *et al.*, *Nucl. Instrum. Methods. A* 329 (1993) 62.
- ⁷ Particle Data Group, K. Hikasa *et al.*, *Phys. Rev. D* 45 S1 (1993).

⁸ See the following and references therein:

Mark III Collab., D. Coffman *et al.*, Phys. Rev. D 45 (1992) 2196.

⁹ Discussions of the isospin decomposition can be found in Refs. [1]. The branching ratio for $D^0 \rightarrow K^{*-}\pi^+$ was computed using a weighted average of our branching ratios for the two $K^{*-}\pi^+$ decay modes.

TABLES

TABLE I. Dalitz plot fit results for the $D^0 \rightarrow K_s^0 \pi^+ \pi^-$ final state. In Tables I-III, the first error is statistical, the second is systematic, and the third error represents uncertainties in the assumed mixture of contributing ($K\pi$) and ($\pi\pi$) resonances and the ($K\pi$) and ($\pi\pi$) resonance shapes.

Decay mode	Decay fraction	Phase (degrees)	Branching ratio (%) [†]
$K^{*-}\pi^+$	$0.625 \pm 0.036 \pm 0.020 \pm 0.016$	0.0 (fixed)	$5.06 \pm 0.29 \pm 0.50 \pm 0.13$
$K_0^*(1430)^-\pi^+$	$0.109 \pm 0.027 \pm 0.028 \pm 0.009$	$-166 \pm 11 \pm 3 \pm 7$	$0.95 \pm 0.23 \pm 0.26 \pm 0.08$
$\overline{K}^0 \rho^0$	$0.350 \pm 0.028 \pm 0.067 \pm 0.006$	$-136 \pm 6 \pm 2 \pm 2$	$1.89 \pm 0.15 \pm 0.45 \pm 0.03$
$\overline{K}^0 f_0(975)$	$0.068 \pm 0.016 \pm 0.017 \pm 0.004$	$38 \pm 11 \pm 3 \pm 4$	$0.47 \pm 0.11 \pm 0.13 \pm 0.03$
$\overline{K}^0 f_2(1270)$	$0.037 \pm 0.014 \pm 0.017 \pm 0.002$	$-174 \pm 11 \pm 20 \pm 42$	$0.24 \pm 0.09 \pm 0.11 \pm 0.01$
$\overline{K}^0 f_0(1400)$	$0.077 \pm 0.022 \pm 0.029 \pm 0.010$	$-45 \pm 12 \pm 21 \pm 12$	$0.44 \pm 0.13 \pm 0.17 \pm 0.06$
$\chi^2/(\text{dof})$	2.29 (23 dof)		

[†] The first systematic error of our measured branching ratios include the statistical uncertainty in the absolute branching ratio into the respective $D \rightarrow K\pi\pi$ final state taken from Ref. [7].

TABLE II. Dalitz plot fit results for the $D^+ \rightarrow K^-\pi^+\pi^+$ final state.

Decay mode	Decay fraction	Phase (degrees)	Branching ratio (%)
$\overline{K}^{*0}\pi^+$	$0.137 \pm 0.006 \pm 0.008 \pm 0.005$	$48 \pm 2 \pm 1 \pm 1$	$1.64 \pm 0.07 \pm 0.18 \pm 0.06$
$\overline{K}_0^*(1430)^0\pi^+$	$0.284 \pm 0.022 \pm 0.032 \pm 0.049$	$63 \pm 2 \pm 3 \pm 4$	$3.66 \pm 0.28 \pm 0.56 \pm 0.63$
$\overline{K}^*(1680)^0\pi^+$	$0.047 \pm 0.006 \pm 0.002 \pm 0.007$	$73 \pm 4 \pm 16 \pm 7$	$1.46 \pm 0.19 \pm 0.18 \pm 0.22$
Nonresonant	$0.998 \pm 0.037 \pm 0.046 \pm 0.056$	0.0 (fixed)	$7.98 \pm 0.30 \pm 0.83 \pm 0.45$
$\chi^2/(\text{dof})$	3.01 (29 dof)		

TABLE III. Dalitz plot fit results for the $D^0 \rightarrow K^- \pi^+ \pi^0$ final state.

Decay mode	Decay fraction	Phase (degrees)	Branching ratio (%)
$K^- \rho^+$	$0.765 \pm 0.041 \pm 0.022 \pm 0.049$	0.0 (fixed)	$8.64 \pm 0.46 \pm 0.88 \pm 0.55$
$K^{*-} \pi^+$	$0.148 \pm 0.028 \pm 0.049 \pm 0.003$	$162 \pm 10 \pm 7 \pm 4$	$5.02 \pm 0.95 \pm 1.73 \pm 0.10$
$\overline{K}^{*0} \pi^0$	$0.165 \pm 0.031 \pm 0.011 \pm 0.011$	$-2 \pm 12 \pm 23 \pm 2$	$2.80 \pm 0.53 \pm 0.33 \pm 0.19$
Nonresonant	$0.101 \pm 0.033 \pm 0.030 \pm 0.027$	$-122 \pm 10 \pm 21 \pm 3$	$1.14 \pm 0.37 \pm 0.36 \pm 0.31$
$\chi^2/(\text{dof})$	1.59 (24 dof)		

TABLE IV. Comparison of branching ratios (%) for three $D \rightarrow K\pi\pi$ final states.

Decay mode	E687 (this work)	Mark III [2] ^{†††}	E691 [4]	ARGUS [5]
<u>$D^0 \rightarrow \bar{K}^0\pi^+\pi^-$</u>				
$K^{*-}\pi^+$	$5.06 \pm 0.29 \pm 0.50 \pm 0.13$	$4.5 \pm 0.3 \pm 0.8$	$3.9 \pm 0.9 \pm 1.0$	5.8 ± 0.7
$K_0^*(1430)^-\pi^+$	$0.95 \pm 0.23 \pm 0.26 \pm 0.08$			1.1 ± 0.4
$\bar{K}^0\rho^0$	$1.89 \pm 0.15 \pm 0.45 \pm 0.03$	$0.8 \pm 0.1 \pm 0.4$	$1.2 \pm 0.3 \pm 0.2$	1.2 ± 0.2
$\bar{K}^0f_0(975)$	$0.47 \pm 0.11 \pm 0.13 \pm 0.03$			0.48 ± 0.20
$\bar{K}^0f_2(1270)$	$0.24 \pm 0.09 \pm 0.11 \pm 0.01$			0.48 ± 0.22
$\bar{K}^0f_0(1400)$	$0.44 \pm 0.13 \pm 0.17 \pm 0.06$			0.71 ± 0.28
Nonresonant		$1.8 \pm 0.3 \pm 0.6$	$1.4 \pm 0.13 \pm 0.22$	
<u>$D^+ \rightarrow K^-\pi^+\pi^+$</u>				
$\bar{K}^{*0}\pi^+$	$1.64 \pm 0.07 \pm 0.18 \pm 0.06$	$1.6 \pm 0.2 \pm 0.9$	$2.0 \pm 0.2 \pm 0.4$	
$\bar{K}_0^*(1430)^0\pi^+$	$3.66 \pm 0.28 \pm 0.56 \pm 0.63$		$3.0 \pm 0.4 \pm 0.2$	
$\bar{K}^*(1680)^0\pi^+$	$1.46 \pm 0.19 \pm 0.18 \pm 0.22$		$0.9 \pm 0.2 \pm 0.4$	
Nonresonant	$7.98 \pm 0.30 \pm 0.83 \pm 0.45$	$6.3 \pm 0.5 \pm 1.6$	$6.7 \pm 0.7 \pm 2.2$	
<u>$D^0 \rightarrow K^-\pi^+\pi^0$</u>				
$K^-\rho^+$	$8.64 \pm 0.46 \pm 0.88 \pm 0.55$	$9.2 \pm 0.3 \pm 1.4$	$7.3 \pm 0.8 \pm 1.7$	
$K^{*-}\pi^+$	$5.02 \pm 0.95 \pm 1.73 \pm 0.10$	$4.2 \pm 0.6 \pm 1.3$	$2.8 \pm 0.5 \pm 0.4$	
$\bar{K}^{*0}\pi^0$	$2.80 \pm 0.53 \pm 0.33 \pm 0.19$	$2.2 \pm 0.3 \pm 0.6$	$2.4 \pm 0.4 \pm 0.4$	
Nonresonant	$1.14 \pm 0.37 \pm 0.36 \pm 0.31$	$1.0 \pm 0.2 \pm 0.5$	$0.41 \pm 0.04 \pm 0.18$	

^{†††}For comparison purposes we have re-scaled the Mark III results by the new Particle Data Group branching ratios [7] for the respective three-body final states.

TABLE V. Comparison of relative phases (in degrees) for three $D \rightarrow K\pi\pi$ final states. Phases marked by (*) have been rotated so that a common reference mode is used between experiments.

Decay mode	E687 (this work)	Mark III [2] ^{§§§}	E691 [4]	ARGUS [5]
<u>$D^0 \rightarrow \bar{K}^0\pi^+\pi^-$</u>				
$K^{*-}\pi^+$	0 (fixed)	0 (fixed)	0 ± 9 (*)	0 (fixed)
$\bar{K}_0^*(1430)^-\pi^+$	$-166 \pm 11 \pm 3 \pm 7$			-157 ± 12
$\bar{K}^0\rho^0$	$-136 \pm 6 \pm 2 \pm 2$	93 ± 30	-232 ± 12 (*)	-137 ± 7
$\bar{K}^0f_0(975)$	$38 \pm 11 \pm 3 \pm 4$			68 ± 15
$\bar{K}^0f_2(1270)$	$-174 \pm 11 \pm 20 \pm 42$			-166 ± 12
$\bar{K}^0f_0(1400)$	$-45 \pm 12 \pm 21 \pm 12$			-31 ± 15
Nonresonant			-109 (fixed) (*)	
<u>$D^+ \rightarrow K^-\pi^+\pi^+$</u>				
$\bar{K}^{*0}\pi^+$	$48 \pm 2 \pm 1 \pm 1$	105 ± 8	-60 ± 3	
$\bar{K}_0^*(1430)^0\pi^+$	$63 \pm 2 \pm 3 \pm 4$		132 ± 2	
$\bar{K}^*(1680)^0\pi^+$	$73 \pm 4 \pm 16 \pm 7$		-51 ± 4	
Nonresonant	0 (fixed)	0 (fixed)	0 (fixed)	
<u>$D^0 \rightarrow K^-\pi^+\pi^0$</u>				
$K^-\rho^+$	0 (fixed)	0 (fixed)	0 ± 7 (*)	
$K^{*-}\pi^+$	$162 \pm 10 \pm 7 \pm 4$	154 ± 11	-152 ± 9 (*)	
$\bar{K}^{*0}\pi^0$	$-2 \pm 12 \pm 23 \pm 2$	7 ± 7	127 ± 9 (*)	
Nonresonant	$-122 \pm 10 \pm 21 \pm 3$	52 ± 9	-40 (fixed) (*)	

^{§§§}We caution comparing our results for two of the decay modes to Ref. [2]. For $D^0 \rightarrow \bar{K}^0\pi^+\pi^-$, they assumed a nonresonant amplitude added incoherently with the resonant modes. For $D^+ \rightarrow K^-\pi^+\pi^+$, the nonresonant amplitude is given by a (non-uniform) phenomenological description.

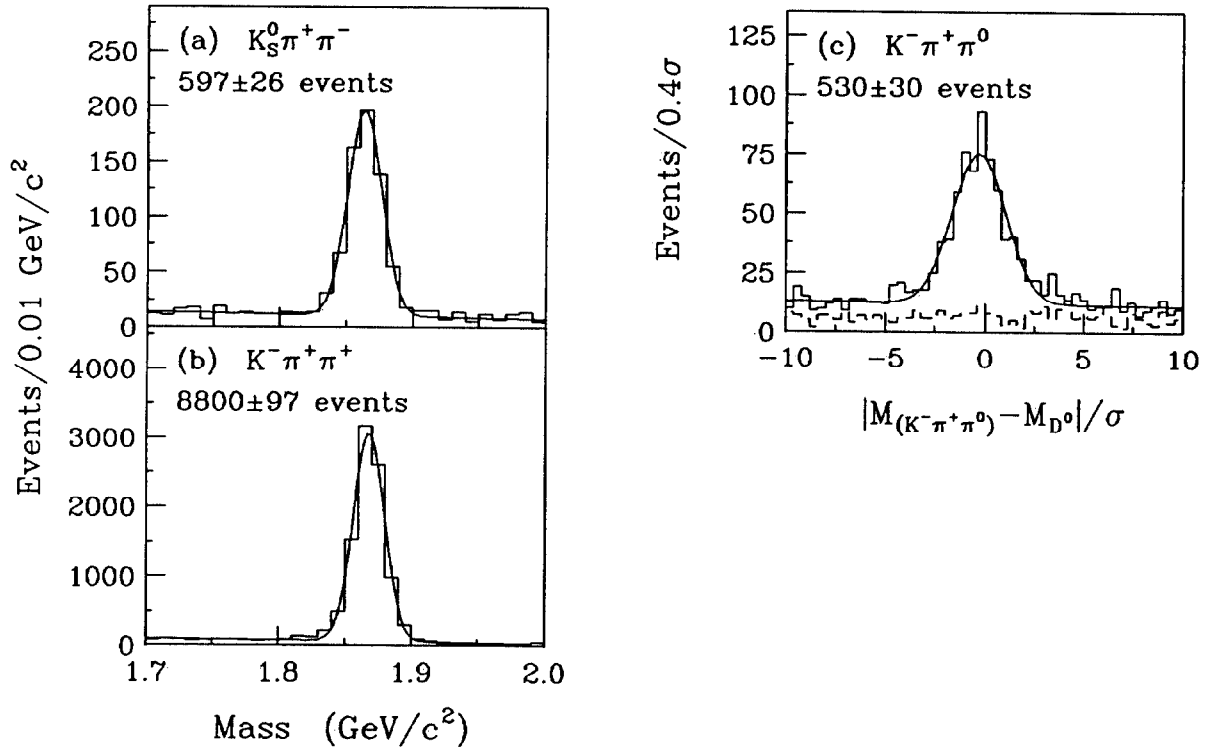


FIG. 1. Invariant mass distributions for the three $D \rightarrow K\pi\pi$ decay modes. In (c) we have plotted the normalized mass difference as defined in the text.

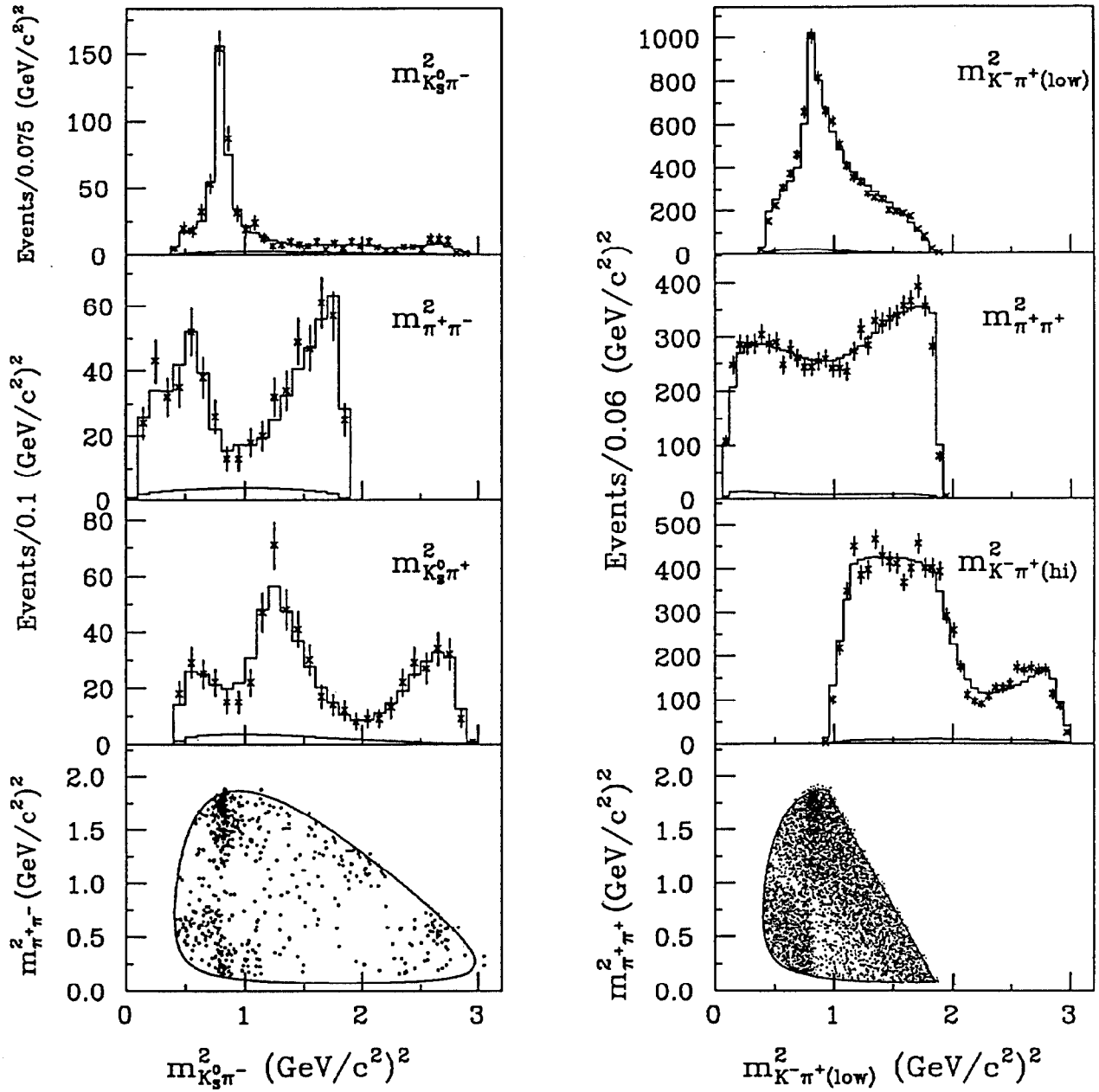


FIG. 2. Dalitz plots and mass-squared projections for the decays $D^0 \rightarrow K_S^0 \pi^+ \pi^-$ and $D^+ \rightarrow K^- \pi^+ \pi^+$. In Figs. 2-3, the data are represented by points, and in each mass-squared projection the upper histogram describes the predicted signal plus background contribution as determined by the fit, and the lower histogram represents the background contribution.

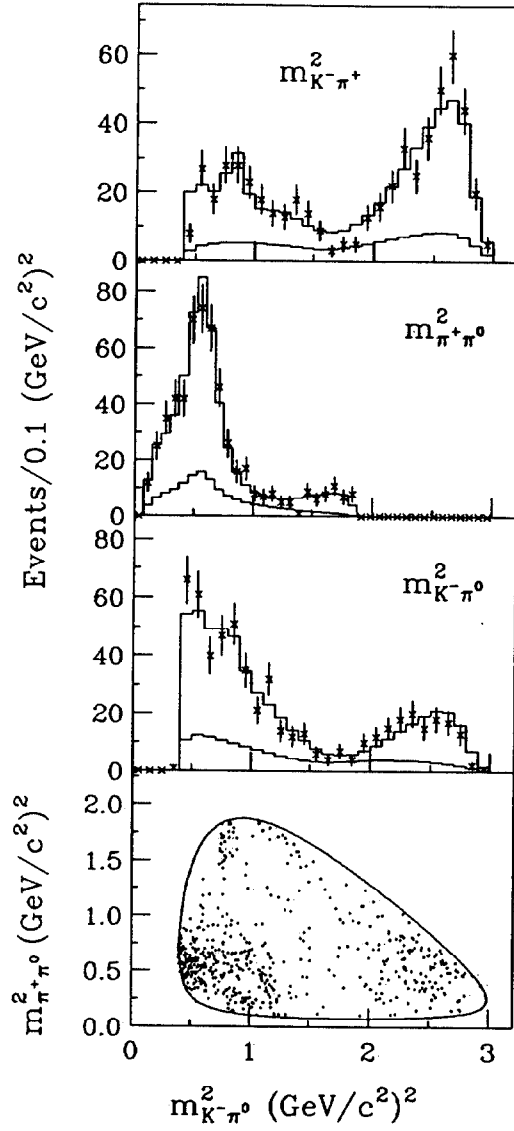


FIG. 3. Dalitz plot and mass-squared projections for the decays $D^0 \rightarrow K^- \pi^+ \pi^0$.